



## Adsorption of $\text{Ca}^{2+}$ and $\text{Mg}^{2+}$ ions from phosphoric acid-nitric acid solution using strong acid cation resin in fixed bed column

Rui Lv<sup>a</sup>, Yingyuan Hu<sup>a</sup>, Rui Li<sup>a</sup>, Xiaochao Zhang<sup>a</sup>, Jianxin Liu<sup>a</sup>, Caimei Fan<sup>a,\*</sup>, Junqiang Feng<sup>b</sup>, Lingyun Zhang<sup>b</sup>, Zhihua Wang<sup>c</sup>

<sup>a</sup>College of Chemistry and Chemical Engineering, Taiyuan University of Technology, Taiyuan 030024, China, Tel. +8613007011210; emails: fancm@163.com (C. Fan), 1281859857@qq.com (R. Lv), 2322629414@qq.com (Y. Hu), 1519146894@qq.com (R. Li), 852355320@qq.com (X. Zhang), 917253881@qq.com (J. Liu)

<sup>b</sup>Shenzhen Batian Ecological Engineering Co. Ltd., Shenzhen 518057, China, email: 2571095296@qq.com (J. Feng), 2283322496@qq.com (L. Zhang)

<sup>c</sup>Tianji Coal Chemical Group Co. Ltd., Changzhi 047507, China, email: 1021489472@qq.com (Z. Wang)

Received 14 October 2018; Accepted 3 February 2019

### ABSTRACT

Adsorption of  $\text{Ca}^{2+}$  and  $\text{Mg}^{2+}$  ions from phosphoric acid-nitric acid solution using strong acid cation resin 001 × 7 has been carried out through fixed bed column and the effects of the dynamic operational parameters, including the feed flow rate, bed height, metal ion concentration, and nitric acid concentration were investigated. Experimental results reveal that the flow rate should be fed at  $1 \text{ mL}\cdot\text{min}^{-1}$ , and the increasing bed height can enhance greatly treatment ability, even for the increasing concentration metal ions.  $7 \text{ mol}\cdot\text{L}^{-1}$  nitric acid solution with the least consumption volume can effectively regenerate the spent resin. Moreover, the dynamic adsorption and elution process remain the steady-status operation during the 10 consecutive processes, which indicates the proposed desalination process is promising for practical application in industrial production of NP fertilizer.

**Keywords:**  $\text{Ca}^{2+}$  and  $\text{Mg}^{2+}$  ions; Strong acid cation resin; Fixed bed column; Consecutive desalination process

### 1. Introduction

Nitrophosphate (NP) fertilizer, as an efficient nitrogen and phosphorus donor, plays important roles in agriculture [1,2]. One common production technology known as the Odds process includes the following steps (Fig. S1): digestion of phosphate rock ( $\text{Ca}_{10}(\text{PO}_4)_6(\text{OH}, \text{F})_2$ ) with nitric acid, separation of acid-insolubles, cooling crystallization, separation of calcium nitrate, mother liquor (the major ingredients: phosphoric acid and nitric acid) neutralization with ammonia gas, evaporation of slurry, granulation, drying, and post-processing of the product [3–5]. Mother liquor neutralization is an important and very complex step in the process of NP fertilizer. The metal ions, particularly

$\text{Ca}^{2+}$  and  $\text{Mg}^{2+}$  ions, existed in the mother liquor always cause many problems [6–8], for example, aggravating viscosity of liquor, increasing the operational difficulty and running cost, reducing the water solubility of fertilizer. Therefore, it is very necessary to remove  $\text{Ca}^{2+}$  and  $\text{Mg}^{2+}$  ions from the mother liquor in the viewpoint of the process requirement as well as fertilizer utilization.

Several methods have been used for the removal of  $\text{Ca}^{2+}$  and  $\text{Mg}^{2+}$  ions such as precipitation [9], extraction [10,11], membrane separation [12], and adsorption [13]. One of the most important methods is adsorption, because of its simple operation, good cycling stability, and easy post treatment [13,14]. Adsorption by the various organic and inorganic polymers such as synthetic resin [15,16],

\* Corresponding author.

carbon materials [17], zeolite [18,19], modified sand [20], and nano-sized hydrogels [21], has been reported. However, for the removal of metal ions from acid solution, strong acid cation (SAC) resin with large adsorption capacity and favorable adsorption characteristic will show the greater potential [22–25]. By means of this material,  $\text{Ca}^{2+}$  and  $\text{Mg}^{2+}$  ions considered as the impurities could be removed from the mother liquor and then eluted by the suitable regeneration solution, which thus achieves the consecutive recycling operation. Furthermore, the nitric acid solution can be designed as the regeneration solution due to its availability in NP fertilizer plant, and when the regeneration ability of the nitric acid solution is exhausted, the solution containing the soluble  $\text{Ca}^{2+}$  and  $\text{Mg}^{2+}$  ions can be used for the production of another fertilizer, such as calcium ammonium nitrate fertilizer [26,27]. For practical purposes, this desalination unit will be significant, because the purification of the mother liquor by SAC resin is really an environment-friendly process, not only solving the troublesome of the neutralization process due to the presence of metal ions, but also promoting the production of water-soluble fertilizers. Therefore, the removal of  $\text{Ca}^{2+}$  and  $\text{Mg}^{2+}$  ions by SAC resin will have great prospects in the production of NP fertilizer.

Knudsen first proposed the method using the ion exchange resin as the new production technology for the NPK fertilizer [28]. Lim and Jørgensen reported a study on modeling, simulation, and optimization to the ion-exchange simulated-moving-bed process for the production of NPK fertilizer [29]. Nevertheless, for the application of SAC resin on the production of NP fertilizer, especially removal of  $\text{Ca}^{2+}$  and  $\text{Mg}^{2+}$  ions from the mother liquor, the study concerning the adsorption equilibrium and the effect of operational parameters has not yet been reported systematically. In our batch experiments the SAC resin 001 × 7 exhibited good adsorption property for  $\text{Ca}^{2+}$  and  $\text{Mg}^{2+}$  ions in phosphoric acid-nitric acid solution, but batch operation is less convenient for the scale-up industrial application, especially for the removal of massive  $\text{Ca}^{2+}$  and  $\text{Mg}^{2+}$  ions. Alternatively, column run is often preferable because of its high yield, excellent recyclability, and ease of operation and handling [30,31]. However, the design and optimization of the fixed bed column cannot be readily obtained from the adsorption equilibrium based on batch study [31]. The effect of operational parameters including the flow rate, bed height and initial ion concentration on the breakthrough characteristics should be further investigated.

Moreover, effective regeneration of saturated resin is another key aspect to guarantee the maximum possible operational capability for desalination process using SAC resin [32]. In this study, nitric acid solution was chosen and used for the regeneration of spent resin column based on practical considerations. And in order to economize the consumption of nitric acid solution and facilitate its post-treatment, the scientific investigation about the effect of the regeneration solution volume and the nitric acid concentration is necessary for the removal of  $\text{Ca}^{2+}$  and  $\text{Mg}^{2+}$  ions from phosphoric acid-nitric acid solution by SAC resin.

Therefore, the aim of this study is to evaluate the performance of 001 × 7 resin on the removal of  $\text{Ca}^{2+}$  and  $\text{Mg}^{2+}$  ions from phosphoric acid-nitric acid solution through the fixed bed column. First, the dynamic removal of metal ions at different operational parameters was performed, including

the feed flow rate, bed height, and initial ion concentration, and Thomas model was used to model the breakthrough curves of the resin column. Subsequently, the effect of the nitric acid concentration and regeneration solution volume on the elution curves for spent resin column was investigated. Finally, the consecutive adsorption-elution process was designed and run 10 cycles to provide the reliable basic data for practical applications of NP fertilizer process.

## 2. Experimental setup

### 2.1. Materials and chemicals

The SAC resin 001 × 7 was obtained from Tianjin Fu Chen Chemical Reagent Factory of China and its specifications were shown in Table S1. Prior to use, the resin was firstly dipped in deionized water for 24 h, then in 4 wt% NaOH solution for 4 h, and finally in 4 wt%  $\text{HNO}_3$  solution for 4 h, respectively, and after each dip, resin was washed with deionized water until the resulting water became neutral, and finally dipped in deionized water.

The synthetic acidic solutions, that were phosphoric acid-nitric acid solutions containing certain  $\text{Ca}^{2+}$  and  $\text{Mg}^{2+}$  ions, were prepared by the analytical grade  $\text{Ca}(\text{NO}_3)_2 \cdot 4\text{H}_2\text{O}$ ,  $\text{Mg}(\text{NO}_3)_2 \cdot 6\text{H}_2\text{O}$ , 65 wt%  $\text{HNO}_3$ , and 85 wt%  $\text{H}_3\text{PO}_4$ , presenting a series of synthetic acidic solutions containing 1.1 mol·L<sup>-1</sup>  $\text{HNO}_3$ , 4.4 mol·L<sup>-1</sup>  $\text{H}_3\text{PO}_4$ , certain  $\text{Ca}^{2+}$  ion concentration (0.15–0.35 mol·L<sup>-1</sup>), and certain  $\text{Mg}^{2+}$  ion concentration (0.15–0.35 mol·L<sup>-1</sup>). The regeneration solutions were nitric acid solutions and were prepared by diluting 65 wt%  $\text{HNO}_3$  with different amount of deionized water.

### 2.2. Dynamic removal of metal ions

The adsorptive removal of single  $\text{Ca}^{2+}$  ion and single  $\text{Mg}^{2+}$  ion from synthetic phosphoric acid-nitric acid solution was carried out in a series of 2 cm inner diameter glass columns with different resin bed heights. The pretreated fresh resin was first loaded into the column and then the synthetic acidic solution was passed through the column upward. Experiments were conducted at different flow rate of synthetic acidic solution (0.5, 1, and 3 mL·min<sup>-1</sup>), bed height (15, 25, and 35 cm), and initial ion concentration (0.15, 0.25 and 0.35 mol·L<sup>-1</sup>). The flow rate was controlled using a peristaltic pump (SHENCHEN, Lab 2015). Samples in the outlet of column were taken at the pre-set time intervals and analyzed for metal ions concentration using atomic-adsorption spectrophotometer (AAS-990).

### 2.3. Regeneration of spent resin

The regeneration study using the nitric acid solution at different concentrations (1–11 mol·L<sup>-1</sup>) was conducted in the glass column (internal diameter: 2 cm, length: 50 cm) packing with 100 g resin. First, the synthetic acidic solution with 0.25 mol·L<sup>-1</sup>  $\text{Ca}^{2+}$  ion and 0.25 mol·L<sup>-1</sup>  $\text{Mg}^{2+}$  ion was passed through the fresh resin column upward at 1 mL·min<sup>-1</sup> flow rate and then the deionized water was fed to the top of the column to rinse the synthetic acidic solution retained. Afterward, the nitric acid solution was flowed through the column in up-flow mode at 1 mL·min<sup>-1</sup> flow rate. The samples in the effluent were taken at regular intervals and analyzed with AAS.

#### 2.4. Consecutive adsorption-elution process

Consecutive adsorption-elution studies were performed in the glass column (internal diameter: 2 cm, length: 50 cm) packing with 100 g resin, as described below:

1. The synthetic acidic solution with  $0.25 \text{ mol}\cdot\text{L}^{-1}$   $\text{Ca}^{2+}$  ion and  $0.25 \text{ mol}\cdot\text{L}^{-1}$   $\text{Mg}^{2+}$  ion was passed through the column upward at  $1 \text{ mL}\cdot\text{min}^{-1}$  flow rate. The samples in the effluent were taken at regular intervals and analyzed with AAS.
2. The deionized water was fed to the top of the column to rinse the synthetic acidic solution retained.
3. The  $7 \text{ mol}\cdot\text{L}^{-1}$  nitric acid solution was then flowed through the column in up-flow mode at  $1 \text{ mL}\cdot\text{min}^{-1}$  flow rate. The samples in the effluent were taken at regular intervals and analyzed with AAS.
4. The deionized water was fed to the top of the column to rinse the nitric acid solution retained and adjust pH to neutral. After that, the resin column was ready for the next adsorption process.

#### 2.5. Modeling of dynamic adsorption process

Thomas model was used to predict the breakthrough curve of metal ions in the effluent. This model assumes that the adsorption process matches the Langmuir isotherm and the second-order reversible reaction kinetics, and no axial dispersion occurs [33,34]. The model can be represented by Eq. (1):

$$\frac{C}{C_0} = \frac{1}{1 + \exp\left[\frac{k_T}{Q}(q_0W - C_0V_{out})\right]} \quad (1)$$

where  $C_0$  is the inlet metal concentration ( $\text{mol}\cdot\text{L}^{-1}$ ),  $C$  is the outlet concentration at different effluent volume,  $k_T$  is the Thomas rate constant ( $\text{L}\cdot(\text{mol}\cdot\text{min})^{-1}$ ),  $Q$  is the volumetric flow rate ( $\text{mL}\cdot\text{min}^{-1}$ ),  $q_0$  is the maximum adsorption capacity of metal ion per unit mass of resin ( $\text{mmol}\cdot\text{g}^{-1}$ ),  $W$  is the resin dosage in the fixed bed column (g),  $V_{out}$  is the effluent volume (mL).

### 3. Results and discussion

#### 3.1. Effect of the operational parameters on adsorption removal of single metal ion

Prior to the investigation, we first need to understand the effect of the feed flow mode on the breakthrough behaviors of single  $\text{Ca}^{2+}$  ion and single  $\text{Mg}^{2+}$  ion in the synthetic acidic solution through the fixed bed resin column. The result in Fig. S2 reveal that the adsorptive removal of metal ion in the up-flow mode provides the better performance. Thus, in the following experiments, the synthetic acidic solution was passed through the resin column upward as described in the experimental section 2.2.

The operational parameters of the dynamic desalination process are very important for the effective removal of ion from solution. In order to investigate the effect of operational parameters on the dynamic adsorption of single  $\text{Ca}^{2+}$  ion and single  $\text{Mg}^{2+}$  ion on resin from the synthetic acidic solution, three set experiments concerning the flow rate, bed height, and initial ion concentration were designed and the results are presented in Figs. 1–3. The breakthrough curves of metal ions were described by Thomas model and the calculated model parameters are listed in Table 1.

Fig. 1 and S3 show the effect of flow rate on the breakthrough curves. From Fig. S3 it can be seen that with the flow rate increasing the treatment rate of the resin column for the adsorption of metal ion in the synthetic acidic solution increases dramatically, but its adsorption efficiency presents the significant variation. As shown in Fig. 1, the break point ( $C/C_0 > 0$ ) of metal ions appears at the less volume while the saturation point ( $C/C_0 = 1$ ) appears at the larger volume. This is because when the flow rate is increased the residence time of the synthetic acidic solution in the resin column will decrease, which thus leads to less effective diffusion of metal ion on resin [16,35]. Nevertheless, the adsorption capacity  $q_0$  calculated by the Thomas model fitting merely presents the slight changing,  $0.64\text{--}0.70 \text{ mmol}\cdot\text{g}^{-1}$  for  $\text{Ca}^{2+}$  ion and  $0.57\text{--}0.64 \text{ mmol}\cdot\text{g}^{-1}$  for  $\text{Mg}^{2+}$  ion. Based on these results,  $1 \text{ mL}\cdot\text{min}^{-1}$  flow rate of synthetic acidic solution was chosen for the subsequent experiments in this study.

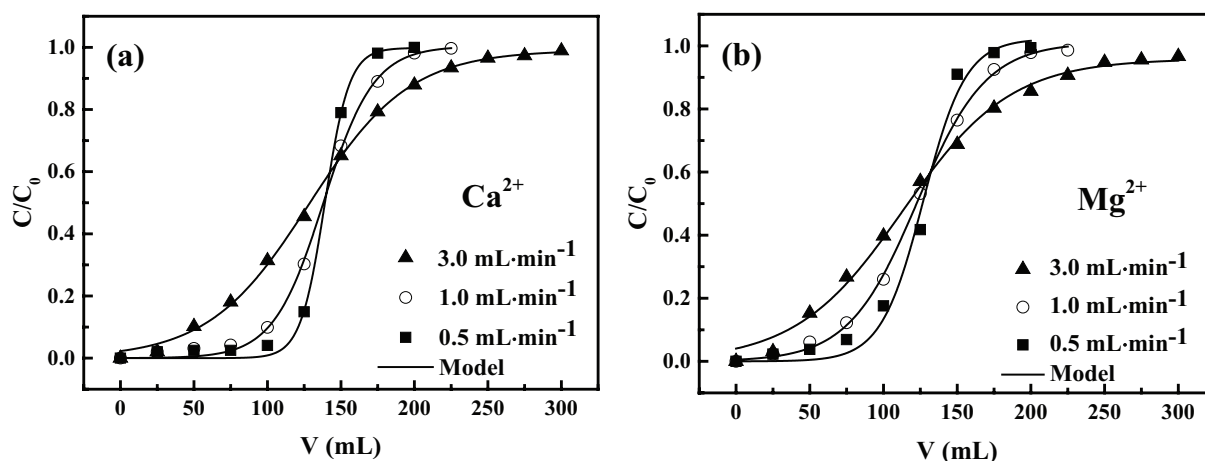


Fig. 1. Breakthrough behaviors of single  $\text{Ca}^{2+}$  ion (a) and single  $\text{Mg}^{2+}$  ion (b) in the synthetic acidic solution at different feed flow rates,  $0.25 \text{ mol}\cdot\text{L}^{-1}$  of initial ion concentration, 25 cm bed height.

Table 1

Fitting results of Thomas model for the dynamic removal of single  $\text{Ca}^{2+}$  ion and single  $\text{Mg}^{2+}$  ion from the synthetic acidic solution in fixed bed column at different operational parameters

Parameters	$R^2$		$k_T/L \cdot (\text{mol} \cdot \text{min})^{-1}$		$q_0/\text{mmol} \cdot \text{g}^{-1}$	
	$\text{Ca}^{2+}$	$\text{Mg}^{2+}$	$\text{Ca}^{2+}$	$\text{Mg}^{2+}$	$\text{Ca}^{2+}$	$\text{Mg}^{2+}$
Flow rate/ $\text{mL} \cdot \text{min}^{-1}$ ( $C_0 = 0.25 \text{ mol} \cdot \text{L}^{-1}$ , bed height = 25 cm)						
0.5	0.998	0.989	0.20	0.14	0.70	0.64
1.0	0.999	0.999	0.23	0.17	0.69	0.61
3.0	0.999	0.996	0.35	0.33	0.64	0.57
Bed height/ cm ( $C_0 = 0.25 \text{ mol} \cdot \text{L}^{-1}$ , flow rate = 1 $\text{mL} \cdot \text{min}^{-1}$ )						
15	0.998	0.996	0.27	0.18	0.70	0.63
25	0.999	0.999	0.23	0.17	0.69	0.61
35	0.998	0.998	0.20	0.16	0.69	0.62
$C_0/\text{mol} \cdot \text{L}^{-1}$ (bed height = 25 cm, flow rate = 1 $\text{mL} \cdot \text{min}^{-1}$ )						
0.15	0.999	0.999	0.31	0.23	0.53	0.45
0.25	0.999	0.999	0.23	0.17	0.69	0.61
0.35	0.999	0.998	0.15	0.12	0.82	0.74

The effect of bed height on the breakthrough curves is shown in Fig. 2. With resin column height increasing, the treatment ability of the resin column will greatly increase. As shown in Fig. 2, both the break point and the saturated point appear at the larger effluent volume. Meanwhile, the  $q_0$  values for the different bed height resin column almost not change (Table 1). These indicate the higher bed height as the result of the increasing resin packing dosage will provide a broadened mass transfer zone for the adsorption of metal ion, and the adsorption equilibrium of metal ion on resin do not be affected, which further suggests the applicability of the fixed bed column in the removal of massive  $\text{Ca}^{2+}$  and  $\text{Mg}^{2+}$  ions from the phosphoric acid-nitric acid solution.

The effect of initial ion concentration on the breakthrough curves is shown in Fig. 3. The results reveal that the treatment ability of the resin column will slightly reduce with the initial ion concentration increasing. Concretely, both the break point and the saturated point for the resin column occur at the less effluent volume. This is because the higher concentration gradient of metal ion will generate the larger mass transfer driving force and thus make the exchange sites on resin exhausted earlier [36,37]. Furthermore, the  $q_0$  values

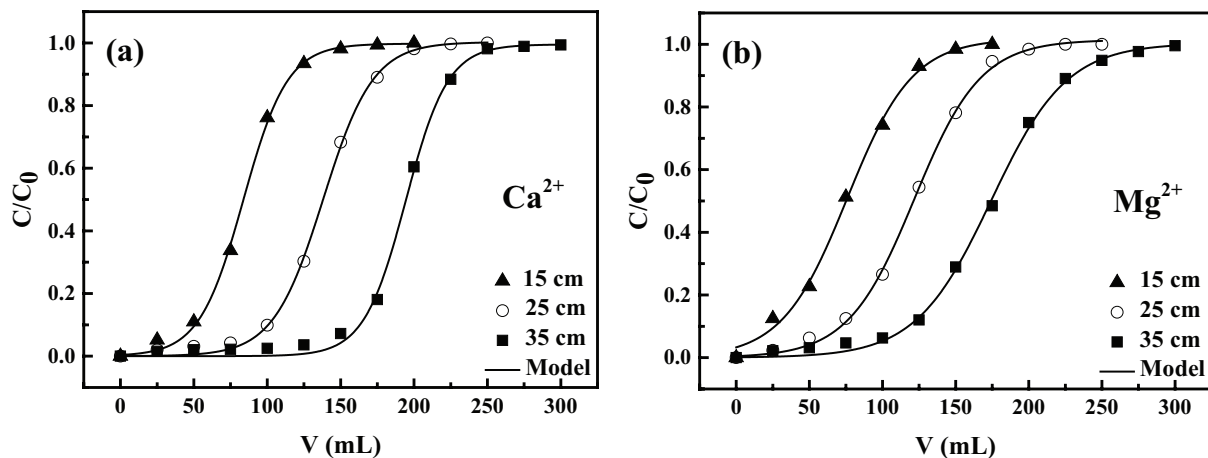


Fig. 2. Breakthrough behaviors of single  $\text{Ca}^{2+}$  ion (a) and single  $\text{Mg}^{2+}$  ion (b) in the synthetic acidic solution at different bed heights, 1  $\text{mL} \cdot \text{min}^{-1}$  of flow rate, 0.25  $\text{mol} \cdot \text{L}^{-1}$  of initial ion concentration.

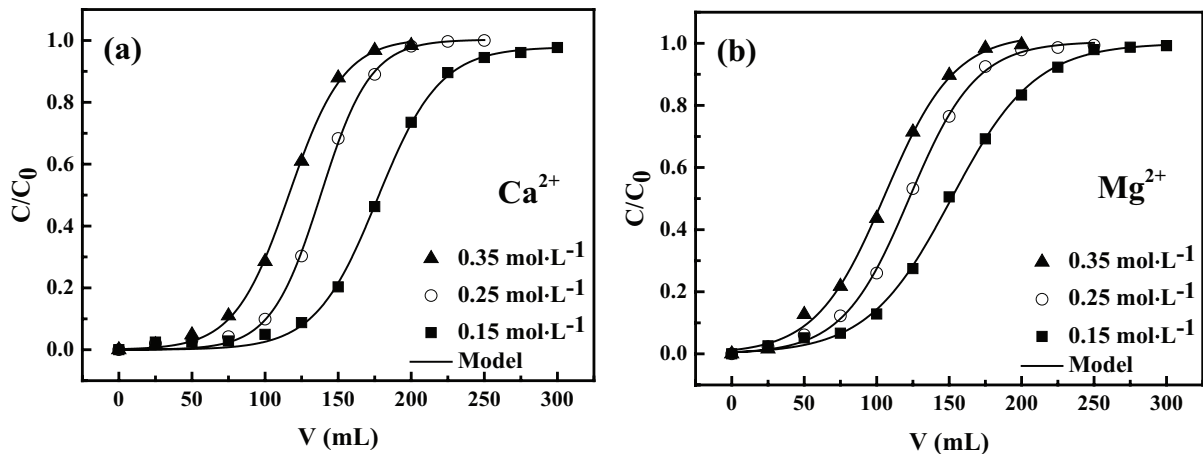


Fig. 3. Breakthrough behaviors of single  $\text{Ca}^{2+}$  ion (a) and single  $\text{Mg}^{2+}$  ion (b) in the synthetic acidic solution at different initial metal ion concentrations, 1  $\text{mL} \cdot \text{min}^{-1}$  of flow rate, 25 cm bed height.

also present a gradually increase as the initial metal ion concentration is increased (Table 1), which is because the increasing mass transfer driving force weakened the negative influence of acids and finally results in the greater number of covered exchange sites. Therefore, it can be concluded that with the metal ion concentration increasing the treated feed volume will decrease, but the adsorption quantities of metal ion on resin will increase.

The fitting results by Thomas model are very closely with the experimental data, and the correlation coefficients ( $R^2$ ) are larger than 0.99. Therefore, Thomas model is very suitable for describing our dynamic adsorption process of  $\text{Ca}^{2+}$  ion or  $\text{Mg}^{2+}$  ion on resin.

Besides, it should be noted that the resin column presents the higher treatment ability for  $\text{Ca}^{2+}$  ion than  $\text{Mg}^{2+}$  ion, both the break point and the saturated point occur at the larger effluent volume, and  $q_0$  values in Table 1 also present the higher values. This difference is due to the higher adsorption affinity of resin toward  $\text{Ca}^{2+}$  ion. Actually, the affinity of resin is toward metal ion with the greater ionic radius, which has the lower hydration energy and thus has the greater tendency to migrate into the resin [20,22].

### 3.2. Simultaneous adsorptive removal of $\text{Ca}^{2+}$ and $\text{Mg}^{2+}$ ions

Based on the earlier results, the simultaneous adsorptive removal of  $\text{Ca}^{2+}$  and  $\text{Mg}^{2+}$  ions from the synthetic acidic solution was studied and used to further testify the feasibility of the proposed desalination process for the practical application. The breakthrough characteristic of metal ions is shown in Fig. 4. As shown in Fig. 4(a), the successful adsorptive removal of metal ions from the synthetic acidic solution has been achieved, and compared with the breakthrough curves of single  $\text{Ca}^{2+}$  ion and single  $\text{Mg}^{2+}$  ion (Figs. 1–3), their respective breakthrough curves in Fig. 4(b) also display the better performance, both the break point and the saturated point appear at the larger effluent volume. The  $q_0$  values calculated by the Thomas model in Table 2 are in good consistent with the observed breakthrough characteristic. The total  $q_0$  value of  $0.93 \text{ mmol}\cdot\text{g}^{-1}$  in 100 g resin column is larger than the value of  $0.69$  or  $0.61 \text{ mmol}\cdot\text{g}^{-1}$  for the adsorption of single metal ion in 50 g resin column (Table 1), while the

respective  $q_0$  values of  $0.49$  and  $0.44 \text{ mmol}\cdot\text{g}^{-1}$  for  $\text{Ca}^{2+}$  ion and  $\text{Mg}^{2+}$  ion in 100 g resin column are smaller than ones in 50 g resin column, which mean the respective adsorption capacities of  $\text{Ca}^{2+}$  ion and  $\text{Mg}^{2+}$  ion in 100 g resin column are influenced by the interaction between these two ions, but the adsorption capacities of the total metal ions are larger. These results indicate that the proposed fixed bed resin column is able to undertake the removal of the massive  $\text{Ca}^{2+}$  and  $\text{Mg}^{2+}$  ions in the synthetic acidic solution. Hence in the subsequent experiments, including the regeneration process of spent resin column as well as the consecutive adsorption-elution process, the synthetic acidic solution containing  $0.25 \text{ mol}\cdot\text{L}^{-1}$   $\text{Ca}^{2+}$  ion and  $0.25 \text{ mol}\cdot\text{L}^{-1}$   $\text{Mg}^{2+}$  ion at  $1 \text{ mL}\cdot\text{min}^{-1}$  flow rate was employed to further evaluate the desalination performance of the designed resin column with 50 cm height and 100 g resin loading.

### 3.3. Regeneration of spent resin column

The effective regeneration of spent resin column is the key aspect to guarantee the consecutive operation for the proposed desalination process. Considering the availability of nitric acid in NP fertilizer plant, nitric acid solution was chosen as the regeneration solution. Prior to the regeneration, the effect of the feed flow mode of the nitric acid solution on the elution process was first investigated and shown in Fig. S4. The up-flow mode has the better performance for the desalination process, thus, in the subsequent experiments the regeneration solution was passed through the fixed bed column upward as described in the experimental section 2.3.

Table 2

Fitting results of Thomas model for the dynamic removal of  $\text{Ca}^{2+}$  and  $\text{Mg}^{2+}$  ions from the synthetic acidic solution in fixed bed column,  $1 \text{ mL}\cdot\text{min}^{-1}$  of flow rate, 50 cm bed height,  $0.25 \text{ mol}\cdot\text{L}^{-1}$   $\text{Ca}^{2+}$  ion and  $0.25 \text{ mol}\cdot\text{L}^{-1}$   $\text{Mg}^{2+}$  ion

$R^2$		$k_t/L\cdot(\text{mol}\cdot\text{min})^{-1}$			$q_0/\text{mmol}\cdot\text{g}^{-1}$			
Total	$\text{Ca}^{2+}$	$\text{Mg}^{2+}$	Total	$\text{Ca}^{2+}$	$\text{Mg}^{2+}$	Total	$\text{Ca}^{2+}$	$\text{Mg}^{2+}$
0.998	0.998	0.998	0.09	0.18	0.20	0.93	0.49	0.44

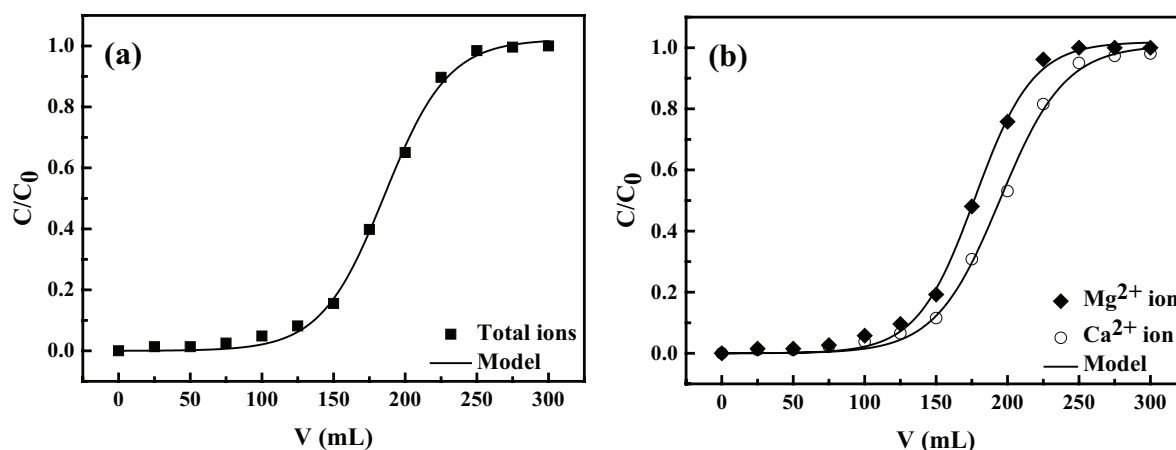


Fig. 4. Breakthrough behaviors of the total metal ions of  $\text{Ca}^{2+}$  and  $\text{Mg}^{2+}$  (a) and the respective  $\text{Ca}^{2+}$  and  $\text{Mg}^{2+}$  (b) in the synthetic acidic solution,  $1 \text{ mL}\cdot\text{min}^{-1}$  of flow rate,  $0.25 \text{ mol}\cdot\text{L}^{-1}$   $\text{Ca}^{2+}$  ion and  $0.25 \text{ mol}\cdot\text{L}^{-1}$   $\text{Mg}^{2+}$  ion, 50 cm bed height.

Nitric acid concentration has an important influence on the regeneration quality of spent resin, the following experiment was designed to study the effect of nitric acid concentrations (1–11 mol·L<sup>-1</sup>) on the regeneration of spent resin, and the elution curves are shown in Fig. 5 and the corresponding elution quantities of metal ions calculated by the elution curves are listed in Table 3. As shown in Table 3, the elution quantities of metal ions increase when the nitric acid concentration increases from 1 to 5 mol·L<sup>-1</sup>, but the elution quantities remain a little change while using the 5–11 mol·L<sup>-1</sup> nitric acid solution, this means that as long as the nitric acid concentration is controlled earlier 5 mol·L<sup>-1</sup> the spent resin column can be efficiently regenerated. Besides, it can be found in Fig. 5(a) that the peak points of elution curve heighten with the nitric acid concentration increasing, and the elution volumes for the complete regeneration lessen. In Fig. 5(b), the peak points of elution curve almost remain unchanged while the elution volumes gradually increase a little bit. These indicate that the nitric acid concentration used in the regeneration process has a suitable value, that is 7 mol·L<sup>-1</sup> nitric acid solution presents the stronger elution ability with the less regeneration solution volume. Thus, considering the more acceptable to the higher concentrated slurry for the post-treatment of exhausted nitric acid solution to produce ammonium nitrate fertilizer, in the consecutive adsorption-elution process, 7 mol·L<sup>-1</sup> nitric acid solution was chosen and used for the regeneration of the spent resin column. Besides, in order to prove the efficiency of elution process, SEM-EDX pattern and elemental mapping of resin ball before and after adsorption of Ca<sup>2+</sup> and Mg<sup>2+</sup> ions in synthetic acidic solution, and after elution using 7 mol·L<sup>-1</sup> nitric acid solution was conducted and is shown in Figs. S5–S7. The SEM-EDX patterns of three resin balls reveal that the elution process can effectively regenerate the spent resin and make it like the fresh resin.

### 3.4. Consecutive desalination process

The consecutive adsorption-elution process was carried out as described in the experimental section 2.4. The adsorption and elution quantities of metal ion in the

consecutive process are shown in Fig. 6, and the breakthrough curves and elution curves are shown in Figs. S8 and S9. The results demonstrate that the adsorption and elution process of Ca<sup>2+</sup> and Mg<sup>2+</sup> ions remain the steady-status operation during the 10 consecutive cycles. As shown in Fig. 6, the adsorption quantities of metal ions by the resin column fluctuate in the range of 0.88–0.92 mmol·g<sup>-1</sup> and the elution quantities of metal ions from the spent resin column undulate in the 0.81–0.95 mmol·g<sup>-1</sup>. Besides both the breakthrough and elution curves for the resin column remain the steady shape within the 10 consecutive operations. Therefore, the proposed desalination process is a reliable operation for the consecutive adsorption-elution of Ca<sup>2+</sup> and Mg<sup>2+</sup> ions from the synthetic acidic solution. In addition, the process 1 including adsorption and elution presents some difference from the following 2–10 processes due to the effect of the resin status [38]. In adsorption process 1, some resin was still Na-type because of the insufficient pretreatment of the acid immersion for the original 001 × 7 resin. After elution process 1, the spent resin in fixed bed column completely was turned into H-type with the nitric acid solution regenerating and the Na-type resin was non-existent for the follow-up 2–10 adsorption processes.

### 3.5. Working principle of the desalination process

The schematic illustration of the working principle for the proposed desalination process is shown in Fig. 7. The yellowish resin ball is first packed in the fixed bed column to carry out the desalination unit. In adsorption process, the synthetic acidic solution containing 0.25 mol·L<sup>-1</sup> Ca<sup>2+</sup> ion and 0.25 mol·L<sup>-1</sup> Mg<sup>2+</sup> ion is continuously passed through the fixed bed column in the up-flow mode. After the resin in column is spent, 7 mol·L<sup>-1</sup> nitric acid solution is continuously

Table 3

Elution quantities of metal ions calculated by the elution curves

Concentration (mol·L <sup>-1</sup> )	1	3	5	7	9	11
Elution quantities (mmol)	59.0	83.9	90.4	88.6	88.5	85.0

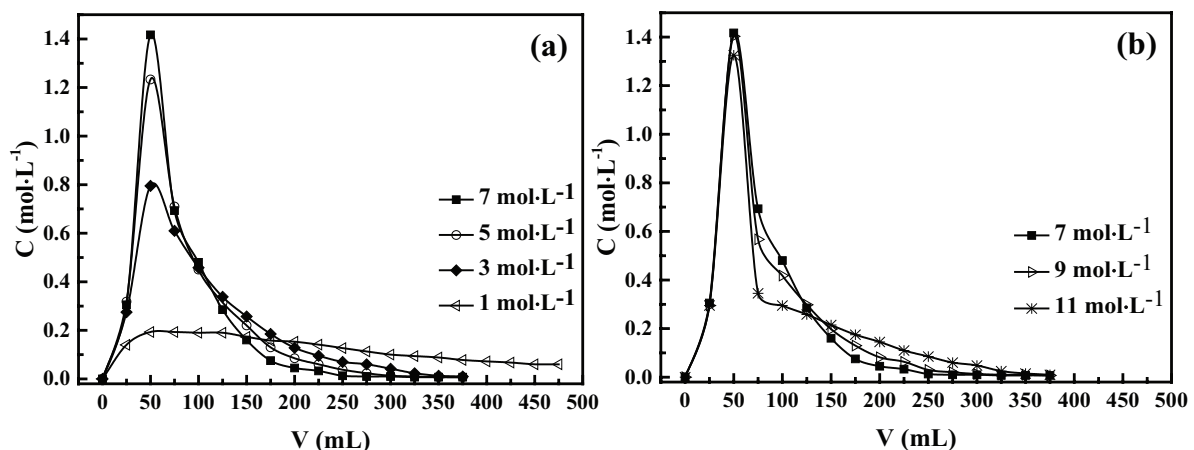


Fig. 5. Regeneration of spent resin with different concentration nitric acid solutions, 1 mL·min<sup>-1</sup> of flow rate, 50 cm bed height, 0.25 mol·L<sup>-1</sup> Ca<sup>2+</sup> ion and 0.25 mol·L<sup>-1</sup> Mg<sup>2+</sup> ion in synthetic acidic solution.

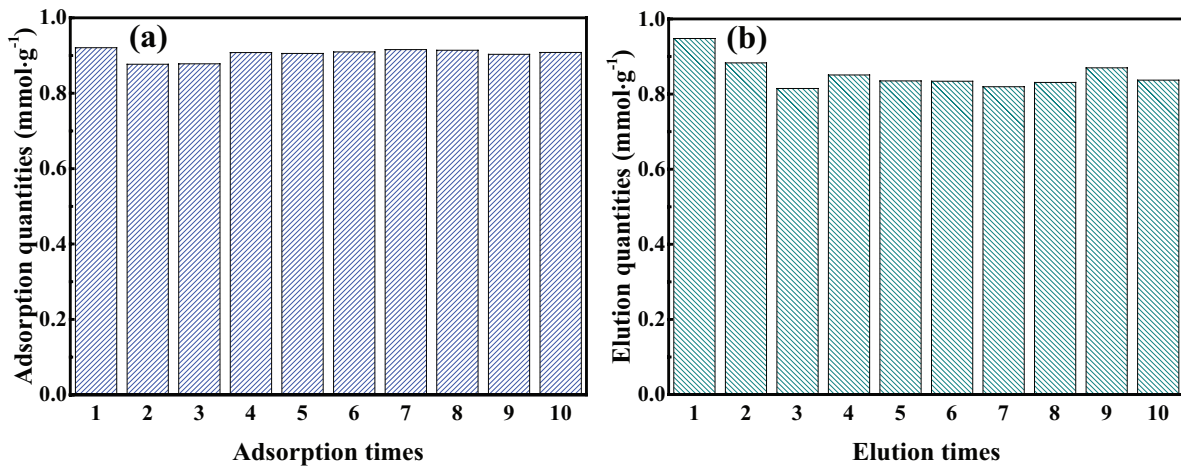


Fig. 6. Adsorption (a) and elution (b) quantities of metal ions in 10 consecutive adsorption-elution process, 1 mL·min<sup>-1</sup> of flow rate, 50 cm bed height, 0.25 mol·L<sup>-1</sup> Ca<sup>2+</sup> ion and 0.25 mol·L<sup>-1</sup> Mg<sup>2+</sup> ion in synthetic acidic solution, 7 mol·L<sup>-1</sup> of nitric acid regeneration solution.

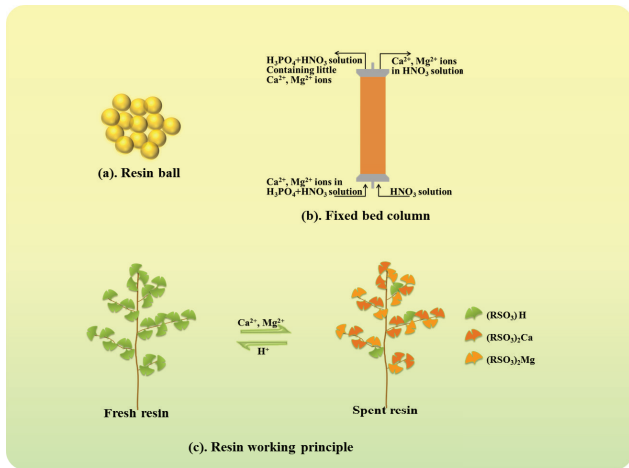
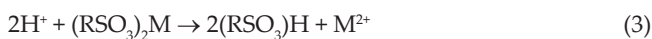
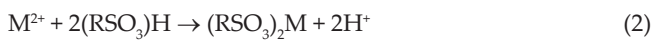


Fig. 7. Schematic illustration of resin ball (a), fixed bed column (b), and the resin working principle for the consecutive adsorption-elution of Ca<sup>2+</sup> and Mg<sup>2+</sup> ions (c).

flowed through the column in up-flow mode until the resin is completely regenerated. Afterward, the resin column is ready to be used for the next adsorption process. The recycling mechanism of resin for the consecutive adsorption-elution of Ca<sup>2+</sup> and Mg<sup>2+</sup> ions are expressed by following Eqs. (2) and (3):



As shown in Eq. (2), for the adsorption process, the metal ions (M<sup>2+</sup>) in the synthetic acidic solution combine with the sulfonic acid group on resin (RSO<sub>3</sub><sup>-</sup>) and the two hydrogen ions are released. While in the elution process, as shown in Eq. (3), the hydrogen ion in the nitric acid solution displaces the metal ions adsorbed on resin and makes the spent resin turn into the active state for the next adsorption process, Fig. 7(c) shows the physical model image of resin working.

#### 4. Conclusions

This study demonstrates that the strong acid cation exchange resin 001 × 7 has the potential to be applied in the removal of Ca<sup>2+</sup> and Mg<sup>2+</sup> ions from phosphoric acid-nitric acid solution through a fixed bed column due to its excellent adsorption-elution properties, and it almost unchanged dynamic adsorption-desorption curves during 10 consecutive adsorption-elution processes. For the synthetic acidic solution containing 0.25 mol·L<sup>-1</sup> Ca<sup>2+</sup> ion and 0.25 mol·L<sup>-1</sup> Mg<sup>2+</sup> ion, the operating conditions of the adsorption process were of 1 mL·min<sup>-1</sup> flow rate and up-flow mode of the synthetic acidic solution, 100 g resin in 50 cm height column with 2 cm inner diameter. Moreover, available nitric acid solution is a suitable and efficient regenerating liquid, the Ca<sup>2+</sup> and Mg<sup>2+</sup> ions adsorbed on the resin could be almost completely regenerated by 7 mol·L<sup>-1</sup> of the nitric acid solution at 1 mL·min<sup>-1</sup> of flow rate through the corresponding resin column.

Note that this study only introduced the Ca<sup>2+</sup> and Mg<sup>2+</sup> ions in the synthetic phosphoric acid-nitric acid solution. In fact there still is a small amount of Fe<sup>3+</sup> and Al<sup>3+</sup> ions in practical mother liquor. The influence of Fe<sup>3+</sup> and Al<sup>3+</sup> ions on the removal of Ca<sup>2+</sup> and Mg<sup>2+</sup> ions by SAC resin 001 × 7 will be investigated in our subsequent study.

#### Acknowledgements

The work described in this paper was substantially supported by a grant from Tianji Coal Chemical Group Co. Ltd. (Project no. 2012–1978) and Shenzhen Batian Ecological Engineering Co., Ltd. (Project no. 2013–0909).

#### Symbols

- C – Outlet concentration
- C<sub>0</sub> – Inlet metal concentration
- H – Hydrogen ion
- k<sub>T</sub> – Thomas rate constant
- M – Metal ions
- Q – Volumetric flow rate
- q<sub>0</sub> – Maximum adsorption capacity of metal ion per unit mass of resin

RSO<sub>3</sub> – Sulfonic acid group on resin  
 $V_{out}$  – Effluent volume, mL  
 $W$  – Resin dosage in the fixed bed column

## References

- [1] J.G. Shepherd, S.P. Sohi, K.V. Heal, Optimising the recovery and re-use of phosphorus from wastewater effluent for sustainable fertiliser development, *Water. Res.*, 94 (2016) 155–165.
- [2] Y.N. Zhu, X.H. Zhang, Y.D. Chen, Q.L. Xie, J.K. Lan, M.F. Qian, N. He, A comparative study on the dissolution and solubility of hydroxylapatite and fluorapatite at 25°C and 45°C, *Chem. Geol.*, 268 (2009) 89–96.
- [3] M. Alemrajabi, Á.C. Rasmuson, K. Korkmaz, K. Forsberg, Recovery of rare earth elements from nitrophosphoric acid solutions, *Hydrometallurgy*, 169 (2017) 253–262.
- [4] K. Binnemans, P.T. Jones, B. Blanpain, T.V. Gerven, Y. Pontikes, Towards zero-waste valorisation of rare-earth-containing industrial process residues: a critical review, *J. Cleaner. Prod.*, 99 (2015) 17–38.
- [5] C. Muntean, W. Brandl, A. Iovi, P. Negrea, Studies on the thermal behavior of a complex mineral fertilizer of nitrophosphate type, *Thermochim. Acta.*, 439 (2005) 21–26.
- [6] G.R. Campbell, Y.K. Leong, C.C. Berndt, J.L. Liowa, Ammonium phosphate slurry rheology and particle properties—the influence of Fe (III) and Al (III) impurities, solid concentration and degree of neutralization, *Chem. Eng. Sci.*, 61 (2006) 5856–5866.
- [7] Y.K. Leong, M. Sganzerla, C.C. Berndt, G.R. Campbell, Metal ions solubility in plant phosphoric acid degree of ammonia neutralization and temperature effects, *Ind. Eng. Chem. Res.*, 47 (2008) 1380–1385.
- [8] S.W. Tang, H. Guo, J.K. Ying, B. Liang, Physicochemical properties of acidic ammonium phosphate slurries, *Ind. Eng. Chem. Res.*, 43 (2004) 3194–3199.
- [9] G.M. Ayoub, R.M. Zayyat, M. Al-Hindi, Precipitation softening: a pretreatment process for seawater desalination, *Environ. Sci. Pollut. Res. Int.*, 21 (2014) 2876–2887.
- [10] G. Falcon-Millan, M.P. Gonzalez-Muñoz, A. Durand, J.A. Reyes-Aguilera, T.A. Razo-Lazcano, M. Avila-Rodriguez, Phosphoric acid partition in aqueous two phase systems, *J. Mol. Liq.*, 241 (2017) 967–973.
- [11] D. Zou, Y. Jin, J. Li, Y.Q. Cao, X. Li, Emulsification solvent extraction of phosphoric acid by tri-n-butyl phosphate using a high-speed shearing machine, *Sep. Purif. Technol.*, 172 (2017) 242–250.
- [12] M.P. González, R. Navarro, I. Saucedo, M. Avila, J. Revilla, Ch. Bouchard, Purification of phosphoric acid solutions by reverse osmosis and nanofiltration, *Desalination*, 147 (2002) 315–320.
- [13] M. Naushad, Z.A. ALOthman, G. Sharma, Inamuddin, Kinetics, isotherm and thermodynamic investigations for the adsorption of Co(II) ion onto crystal violet modified amberlite IR-120 resin, *Ionics*, 21 (2015) 1453–1459.
- [14] M. Naushad, G. Sharma, A. Kumar, S. Sharm, A.A. Ghfar, A. Bhatnagar, F.J. Stadler, M.R. Khan, Efficient removal of toxic phosphate anions from aqueous environment using pectin based quaternary amino anion exchanger, *Int. J. Biol. Macromol.*, 106 (2018) 1–10.
- [15] Z.H. Yu, T. Qi, J.K. Qu, L. Wang, J.L. Chu, Removal of Ca(II) and Mg(II) from potassium chromate solution on Amberlite IRC 748 synthetic resin by ion exchange, *J. Hazard. Mater.*, 167 (2009) 406–412.
- [16] W.T. Yi, C.Y. Yan, P.H. Ma, Removal of calcium and magnesium from LiHCO<sub>3</sub> solutions for preparation of high-purity Li<sub>2</sub>CO<sub>3</sub> by ion-exchange resin, *Desalination*, 249 (2009) 729–735.
- [17] L. Monser, M.B. Amor, M. Ksibi, Purification of wet phosphoric acid using modified activated carbon, *Chem. Eng. Process.*, 38 (1999) 267–271.
- [18] Y.H. Liu, W. Ma, Z.H. Cheng, J. Xu, R. Wang, X. Gang, Preparing CNTs/Ca-Selective zeolite composite electrode to remove calcium ions by capacitive deionization, *Desalination*, 326 (2013) 109–114.
- [19] M. Al-Anbera, Z.A. Al-Anber, Utilization of natural zeolite as ion-exchange and sorbent material in the removal of iron, *Desalination*, 225 (2008) 70–81.
- [20] A.A. El-Bayaa, N.A. Badawy, A.M. Gamal, I.H. Zidan, A.R. Mowafy, Purification of wet process phosphoric acid by decreasing iron and uranium using white silica sand, *J. Hazard. Mater.*, 190 (2011), 324–329.
- [21] G. Sharma, B. Thakur, M. Naushad, A. Kumar, F.J. Stadler, S.M. Alfadul, G.T. Mola, Applications of nanocomposite hydrogels for biomedical engineering and environmental protection, *Environ. Chem. Lett.*, 16 (2018) 113–146.
- [22] K.L. Ang, D. Li, A.N. Nikoloski, The effectiveness of ion exchange resins in separating uranium and thorium from rare earth elements in acidic aqueous sulfate media. Part 1. Anionic and cationic resins, *Hydrometallurgy*, 174 (2017) 147–155.
- [23] D.J. Hwang, Y.H. Yu, C.S. Baek, G.M. Lee, K.H. Cho, J.W. Ahn, C. Han, J.D. Lee, Preparation of high purity PCC from medium- and low-grade limestones using the strongly acidic cation exchange resin, *J. Ind. Eng. Chem.*, 30 (2015) 309–321.
- [24] J.P. Michael, S. Karin, D.O. Mark, Comparative study of the application of chelating resins for rare earth recovery, *Hydrometallurgy*, 169 (2017) 275–281.
- [25] G.J. Millar, S.J. Couperthwaite, M.d. Bruyn, C.W. Leung, Ion exchange treatment of saline solutions using Lanxess S108H strong acid cation resin, *Chem. Eng. J.*, 280 (2015) 525–535.
- [26] E.A. Abdel-aal, A.M. Amer, Evaluation of Sebaiya-west phosphate concentrate for nitrophosphate fertilizer production, *Miner. Eng.*, 8 (1995) 1221–1230.
- [27] I. Hussain, The Operating experience of Nitrophosphate Plant, *Procedia. Eng.*, 46 (2012) 172–177.
- [28] K.C. Knudsen, The production of NPK fertilisers by ion exchange, *J. appl. Chem. Biotechnol.*, 24 (1974) 701–708.
- [29] Y.I. Lim, S.B. Jørgensen, Optimization of a six-zone simulated-moving-bed chromatographic process, *Ind. Eng. Chem. Res.*, 46 (2007) 3684–3697.
- [30] K.H. Chu, Improved fixed bed models for metal biosorption, *Chem. Eng. J.*, 97 (2004) 233–239.
- [31] S. Kundu, A.K. Gupta, As(III) removal from aqueous medium in fixed bed using iron oxide-coated cement (IOCC): experimental and modeling studies, *Chem. Eng. J.*, 129 (2007) 123–131.
- [32] M.D. Victor-Ortega, J.M. Ochando-Pulido, A. Martínez-Ferez, Impacts of main parameters on the regeneration process efficiency of several ion exchange resins after final purification of olive mill effluent, *Sep. Purif. Technol.*, 173 (2017) 1–8.
- [33] R.S. Juang, H.C. Kao, W. Chen, Column removal of Ni(II) from synthetic electroplating waste water using a strong-acid resin, *Sep. Purif. Technol.*, 49 (2006) 36–42.
- [34] M.D. Victor-Ortega, J.M. Ochando-Pulido, A. Martínez-Ferez, Iron removal and reuse from Fenton-like pretreated olive mill wastewater with novel strong-acid cation exchange resin fixed-bed column, *J. Ind. Eng. Chem.*, 36 (2016) 298–305.
- [35] J.P. Chen, M.L. Chua, B.P. Zhang, Effects of competitive ions, humic acid, and pH on removal of ammonium and phosphorous from the synthetic industrial effluent by ion exchange resins, *Waste. Manage.*, 22 (2002) 711–719.
- [36] N.H. Shaidan, U. Eldemerdash, S. Awad, Removal of Ni(II) ions from aqueous solutions using fixed-bed ion exchange column technique, *J. Taiwan. Inst. Chem. Eng.*, 43 (2012) 40–45.
- [37] Z.H. Yu, T. Qi, J.K. Qu, Y.C. Guo, Application of mathematical models for ion-exchange removal of calcium ions from potassium chromate solutions by Amberlite IRC 748 resin in a continuous fixed bed column, *Hydrometallurgy*, 158 (2015) 165–171.
- [38] M. Coca, S. Mato, G. González-Benito, M.Á. Uruña, M.T. García-Cubero, Use of weak cation exchange resin Lewatit S 8528 as alternative to strong ion exchange resins for calcium salt removal, *J. Food. Eng.*, 97 (2010) 569–573.

## Supporting information

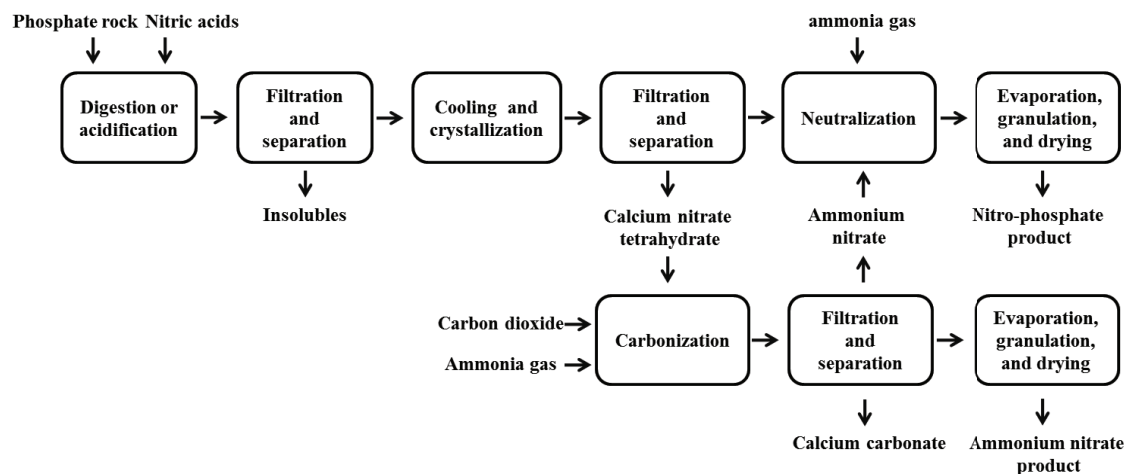


Fig. S1. Overall flow sheet of the Odda process.

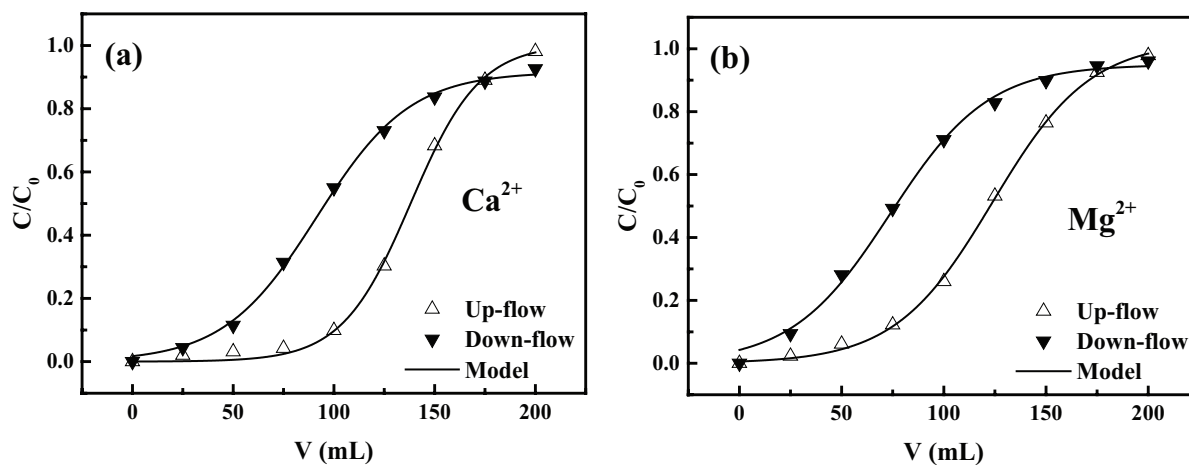


Fig. S2. Breakthrough behaviors of single  $\text{Ca}^{2+}$  ion (a) and single  $\text{Mg}^{2+}$  ion (b) in the synthetic acidic solution at different flow modes,  $1 \text{ mL}\cdot\text{min}^{-1}$  of flow rate,  $0.25 \text{ mol}\cdot\text{L}^{-1}$  of initial ion concentration,  $25 \text{ cm}$  bed height.

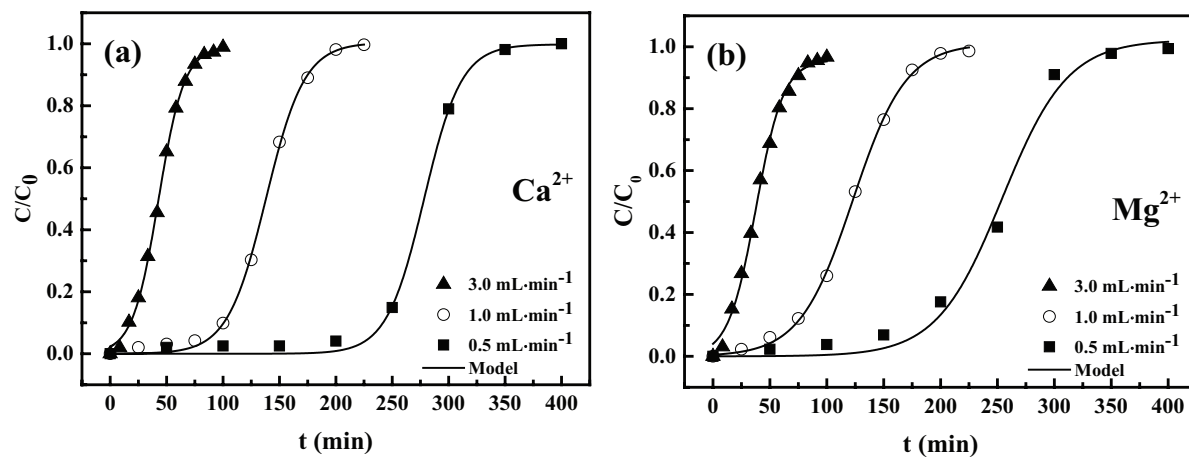


Fig. S3. Breakthrough behaviors of single  $\text{Ca}^{2+}$  ion (a) and single  $\text{Mg}^{2+}$  ion (b) in the synthetic acidic solution at different feed flow rates,  $0.25 \text{ mol}\cdot\text{L}^{-1}$  of initial ion concentration,  $25 \text{ cm}$  bed height.

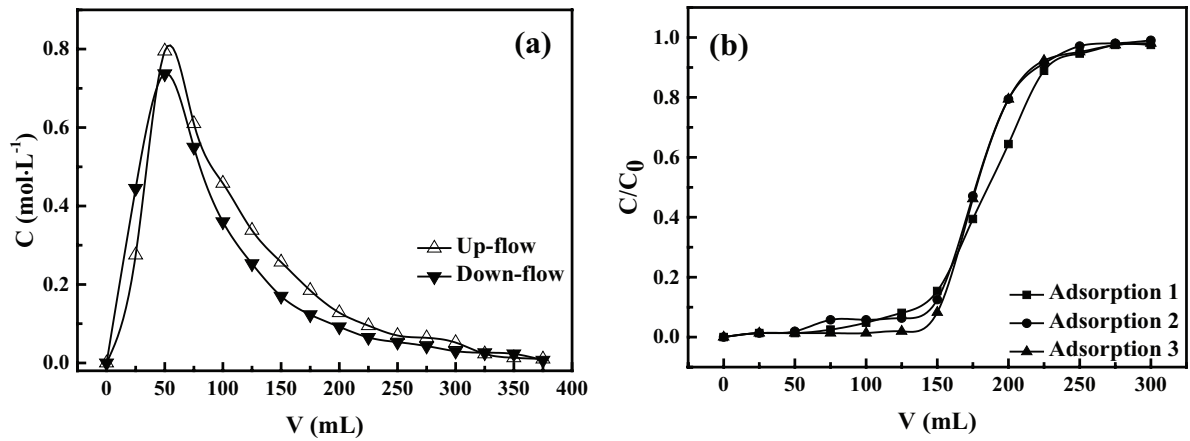


Fig. S4. Effect of the feed flow mode on the elution curves with 3 mol·L<sup>-1</sup> of the nitric acid regeneration solution (a) and the following breakthrough curves of the total metal ion in the synthetic acidic solution with 0.25 mol·L<sup>-1</sup> Ca<sup>2+</sup> ion and 0.25 mol·L<sup>-1</sup> Mg<sup>2+</sup> ion (b), 1 mL·min<sup>-1</sup> of flow rate, 50 cm bed height.

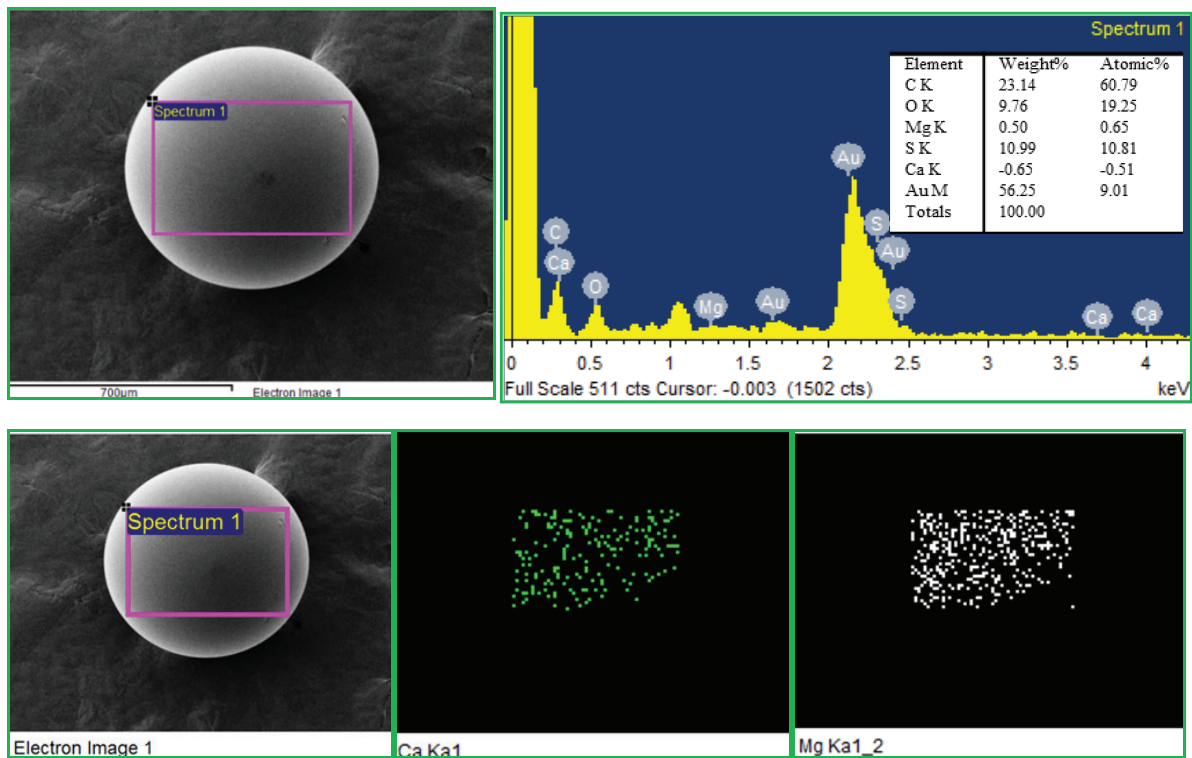


Fig. S5. SEM-EDX pattern and elemental mapping of original resin bell.

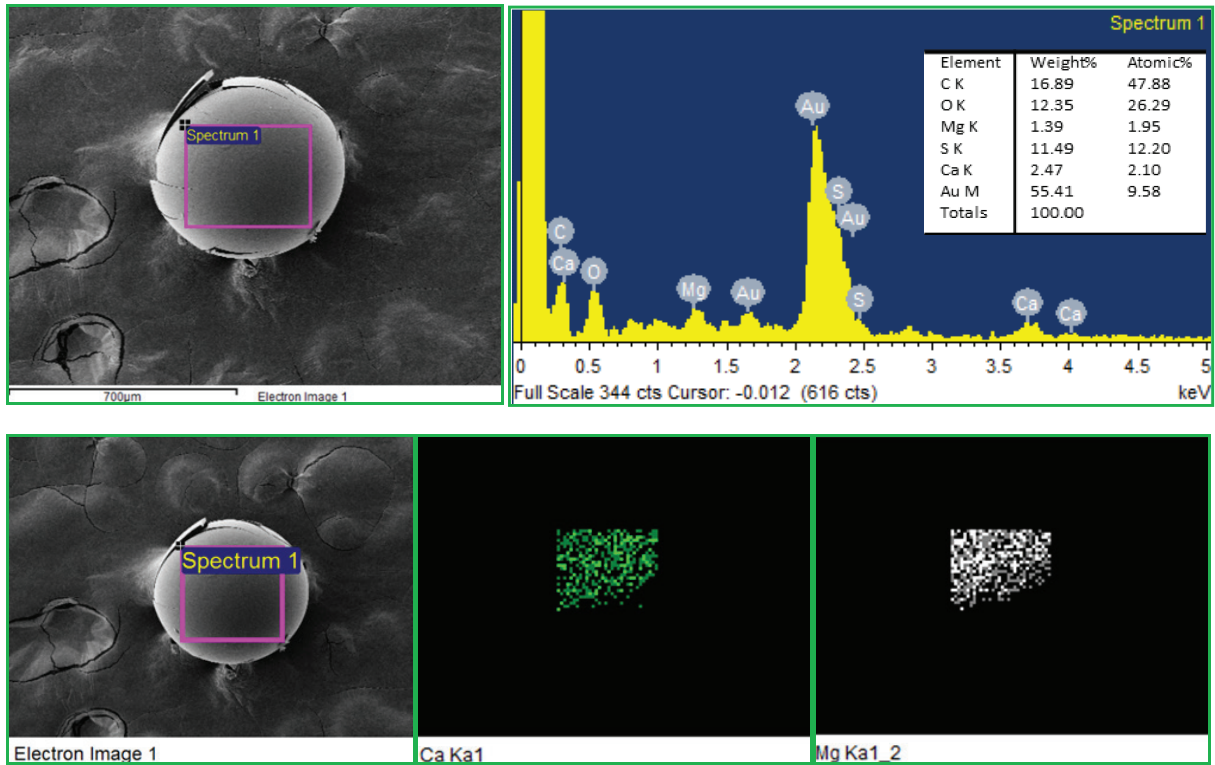


Fig. S6. SEM-EDX pattern and elemental mapping of resin bell after adsorption of  $\text{Ca}^{2+}$  and  $\text{Mg}^{2+}$  ions in synthetic acidic solution.

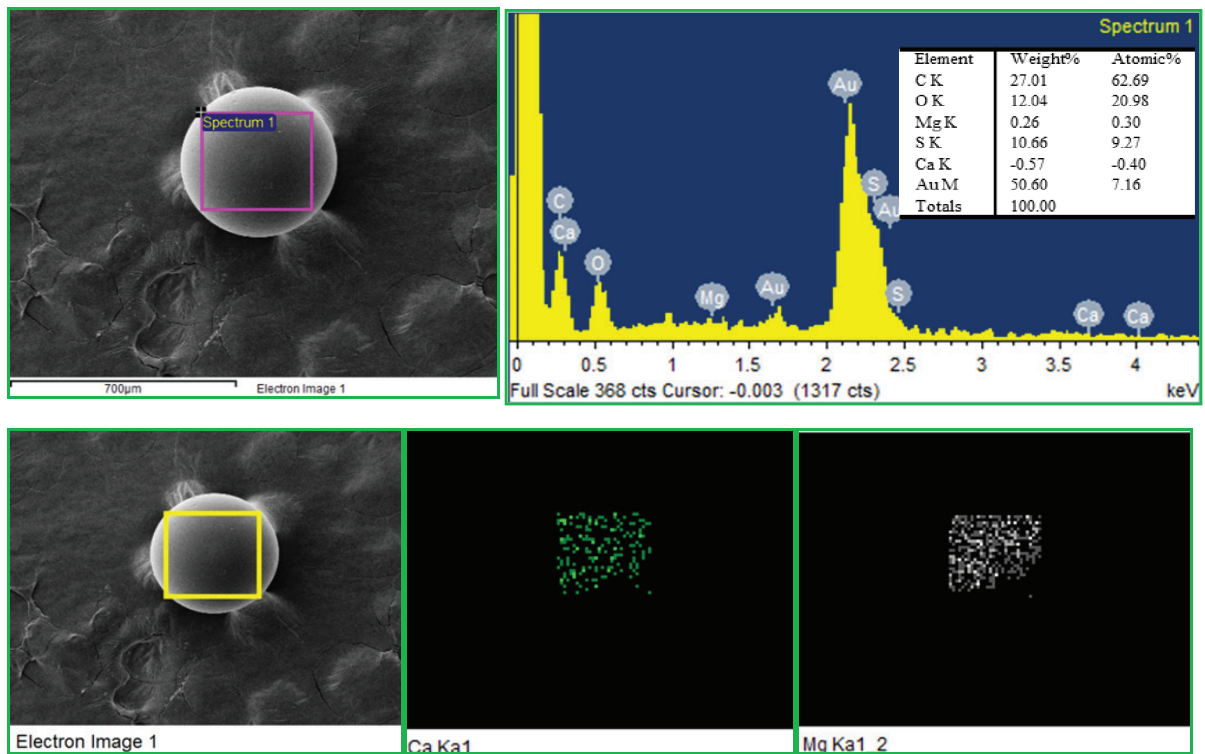


Fig. S7. SEM-EDX pattern and elemental mapping of resin bell after elution by  $7 \text{ mol}\cdot\text{L}^{-1} \text{ HNO}_3$  solution.

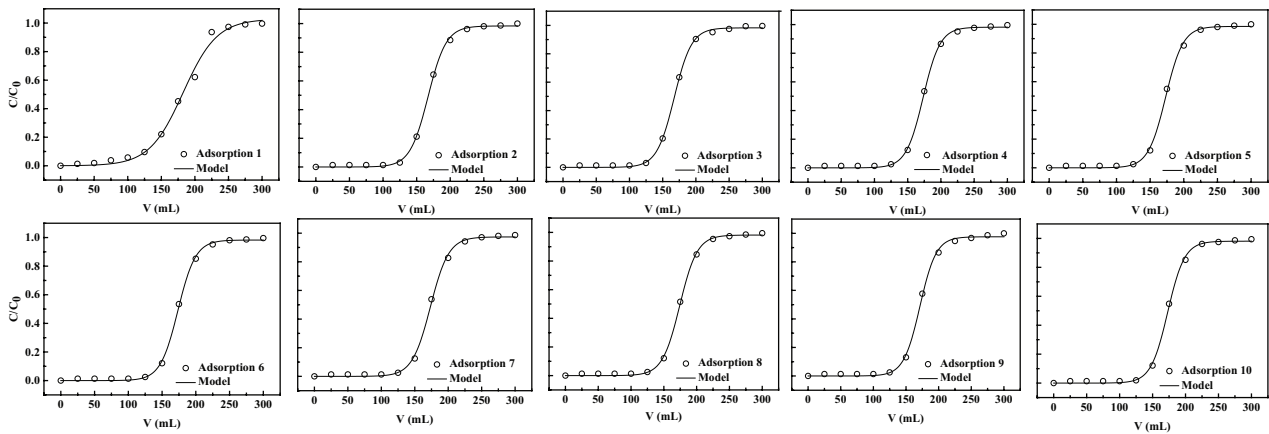


Fig. S8. Breakthrough behaviors of the total metal ions in the synthetic acidic solution during 10 consecutive adsorption-elution process,  $1 \text{ mL}\cdot\text{min}^{-1}$  of flow rate,  $0.25 \text{ mol}\cdot\text{L}^{-1} \text{ Ca}^{2+}$  and  $0.25 \text{ mol}\cdot\text{L}^{-1} \text{ Mg}^{2+}$ , 50 cm bed height.

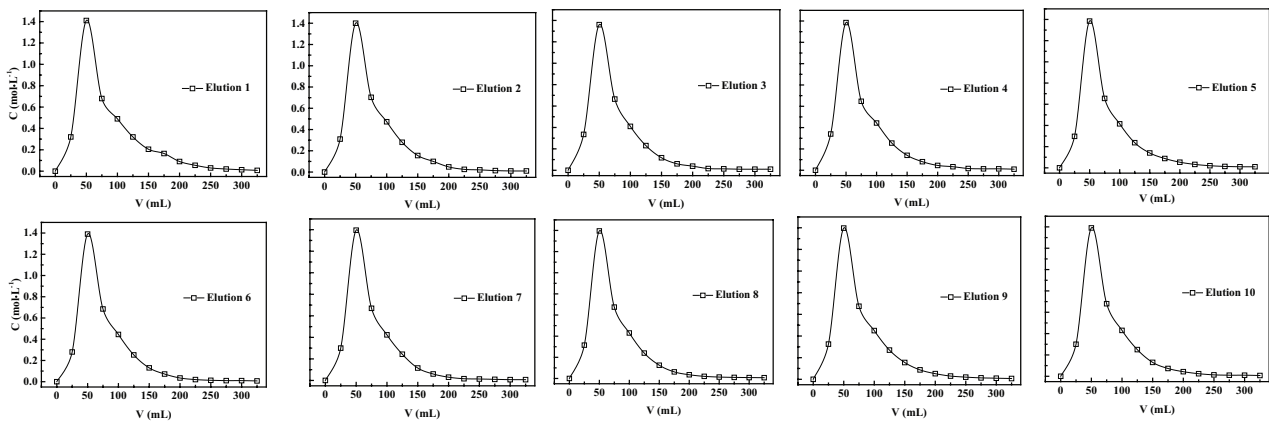


Fig. S9. Elution behaviors of the total metal ion from the spent resin column during 10 consecutive adsorption-elution process,  $1 \text{ mL}\cdot\text{min}^{-1}$  of flow rate,  $7 \text{ mol}\cdot\text{L}^{-1}$  of the nitric acid regeneration solution, 50 cm bed height.

Table S1  
Characteristics of strong acid cation resin  $001 \times 7$  supplied by manufacturer

Characteristics	Values
Matrix	Styrene-divinylbenzene copolymer
Functional groups	Sulphonates
Ionic form as shipped	$\text{Na}^+$
Total exchange capacity	$\geq 1.8 \text{ equiv. L}^{-1}$
Specific gravity	1.23–1.28
Moisture holding capacity	45%–55%
Particle size (0.3~1.2 mm)	$\geq 95\%$
Maximum operating temperature	$120^\circ\text{C}$
pH range	1~14